DISTRIBUTION STATEMENT A. Approved for public release; distribution is unlimited.

Acoustical Characterization of the Riverine Environment

D. Benjamin Reeder
Department of Oceanography
Naval Postgraduate School
833 Dyer Rd.
Monterey, CA 93943
phone: (831) 525-5255 fax: (831) 656-2712 email: dbreeder@nps.edu

Award Number: N0001414WX20439
http://www.oc.nps.edu

LONG-TERM GOALS

Develop a new capability in monitoring, understanding and predicting the dynamics of the riverine environment based on the characterization of the acoustical environment through *in situ* field observations and modeling which are closely linked to environmental measurements.

OBJECTIVES

Define and describe the acoustical characteristics of different riverine environments (e.g. braided (shallow, strong currents, gravelly bed), meandering (deep, weak currents, muddy bed)) using simple acoustic instrumentation, and correlate these acoustical characteristics to traditional riverine observational parameters (e.g. current profiles, geological descriptors).

Develop an acoustic propagation model to investigate the effect of the environment on the measured acoustic parameters, and validate the acoustic model with *in situ* field observations.

Through measurements and modeling, investigate the sensitivity of these acoustical-environmental correlations to frequency, and examine the temporal and spatial scales of variability in the riverine environment and its impact on signal coherence as a function of time, frequency and range.

APPROACH

The focus of the FY14 effort was analysis and associated acoustic propagation modeling of the data collected during the acoustic portion of the RIVET II field experiment at the Mouth of the Columbia River (MCR) estuary in June 2013. 'MCR Acoustics' consisted of a 2-week long cruise on the R/V Oceanus during the latter half of May.

WORK COMPLETED

During the field experiment, multiple instrumented moorings and the tripod were deployed at strategic times and locations indicated in Fig. 1 to facilitate the following objectives: (1) correlate ambient noise and acoustic signature statistics with measured physical parameters (current profiles and surface

conditions); (2) characterize the contribution to the ambient noise environment by shipping traffic; and (3) investigate the acoustic propagation characteristics of the salt wedge. The research effort during FY14 has been focused on (1) analysis of the acoustic transmissions across the shipping channel from the acoustic source deployed over the side of the ship at station S2 and received at the hydrophone at tripod mooring A5 (Fig. 1), (2) modeling the acoustic propagation between S2 and A5 to properly interpret the physical mechanisms, and (3) analysis of the flow noise as a function of current speed and acoustic frequency. Modeling of the acoustic transmissions is based on the environmental input (T&S profiles) from modeling hindcasts generously provided by the Center for Coastal Margin Observation and Prediction (CMOP) for the period of the experiment. Several presentations have been given at program reviews and conferences, and one manuscript is ready for submission to the Journal of the Acoustical Society of America pending updated modeling results.

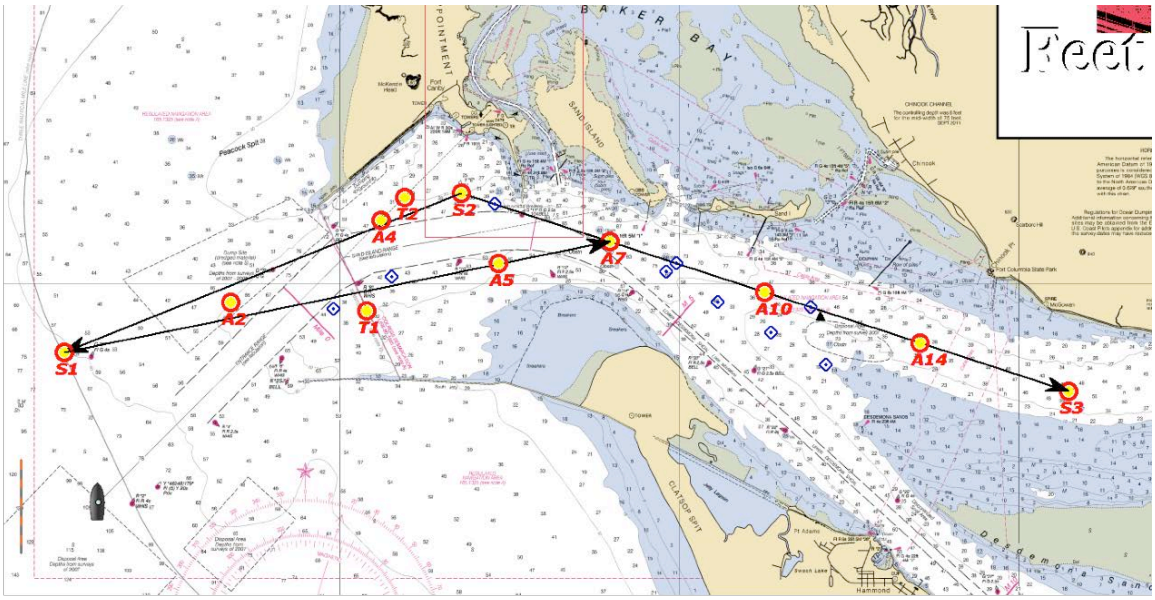

Fig. 1. Mooring laydown geometry during the acoustic portion of the RIVET II field experiment.

RESULTS

Figure 2 shows results from the experiment from 2300 May 28 to 0500 May 29 during ebb tide. The source was deployed at anchor station S2 (north side of channel, halfway between the North Jetty and Jetty A) and the signal was received by the hydrophone on the tripod at mooring station A5 (1.36 km SSE of S2 on the south side of the channel). Two-second long linear frequency-modulated (LFM) signals having a 1500 Hz bandwidth (500-2000 Hz) were transmitted once every 10 seconds for a six hour period. This observation period occurred from the top of the ebb to the bottom of the flood during which the salt wedge front receded from the point of greatest advance upriver of both source and receiver to the point of greatest recession near the mouth downriver of the source and receiver. The bottom panel shows sound speed (m/s) as a function of range (in degrees latitude) and depth (m) along the acoustic path between the source at S2 and the receiver at A5. This across-channel transect is shown looking from west to east into the estuary. The sound speed is based upon T and S profiles provided by CMOP in Portland. The source is depicted on the left at 4 m water depth and the receiver

on the tripod is depicted on the right 1 m above the riverbed. The CMOP model output was provided in 15 minute increments and this particular profile is the one for 0245Z on May 29, which is the approximate time at which the acoustic source occupies the depth of greatest sound speed gradient. The middle panel shows sound speed profiles from CTD data collected on a Castaway CTD hand-deployed over the side of the ship in approximately 15 minute intervals during the acoustic transmission period. Note that as the salt wedge recedes during ebb, 0230 is the approximate time at which the source at 4 m water depth moves from salt water to fresh water. The top panel shows compressed pulse output in terms of relative received signal energy level (SEL) in dB re 1 μPa^2-sec averaged over 60-second moving windows observed at A5 vs. time on the same scale as shown in the middle panel. The SEL is relatively stable prior to 0100Z, steadily decreases 10 dB during a 1 ½ hour period, reaches a minimum at ~0230Z, then rapidly increases 10 dB during a 1 hour period, finally returning at 0330Z to approximately the same level as observed prior to 0100Z. Sound speed varies between 1460 and 1490 m/s primarily due to the salinity variation of 28 psu while temperature varied by only 1.5^{o}C. The sound speed gradient during ebb, while significant, is weaker than during flood, as seen in the next figure.

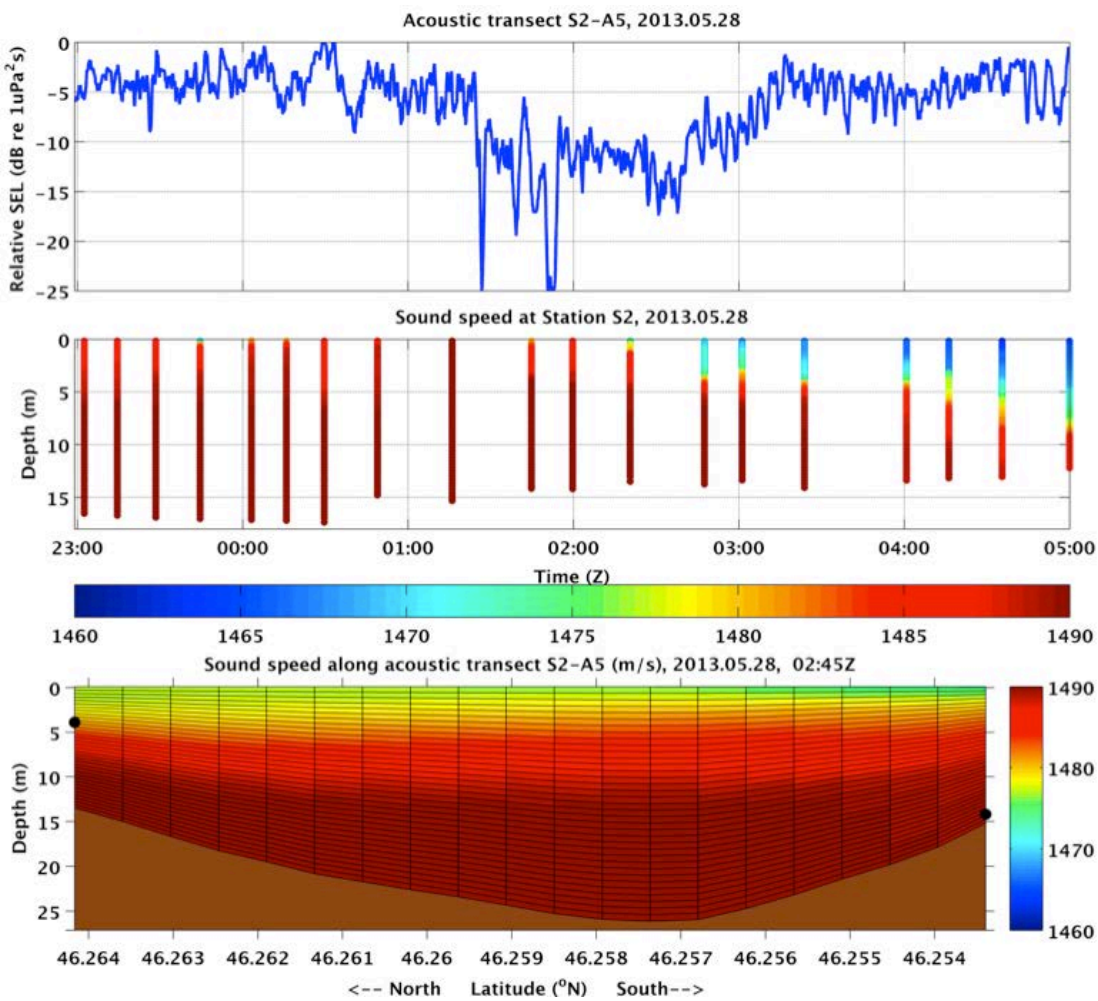

Fig. 2. Ebb from 2300 May 28 to 0500 May 29: (a) Relative SEL (dB re 1 μPa^2-sec) vs. time (hr); (b) sound speed (m/s) vs. depth (m) and time (hr) observed at S2; (c) modeled sound speed (m/s) vs. depth (m) and range (deg. latitude) along the acoustic transect between S2 and A5.

Figure 3 has the same form as Fig. 2 but shows results for the flood on May 27. The bottom panel shows sound speed for the same acoustic transect between S2 and A5, with the acoustic source deployed at 6 m water depth and the receiver in the same location 1 m off the bottom at A5. This CMOP model output timestamp is 1915Z in this case. The middle panel again shows sound speed computed from the Castaway CTD deployed over the side of the ship in approximately 15 min intervals during the acoustic transmission period. Note that the acoustic source at 6 m water depth moves from fresh water to salt water at approximately 1930Z. The top panel shows a relatively stable SEL prior to 1700Z; SEL then slowly decreases approximately 15 dB during a 2 ½ hour period, reaches a minimum at approximately 1930Z, then rapidly increases 15 dB during a 1 hour period, finally returning at 2030Z to approximately the same level as observed prior to 1700Z. As the source enters the salt wedge and the acoustic transect is progressively composed of salt water, the SEL observed at A5 rapidly increases and finally attains its pre-salt wedge passage level.

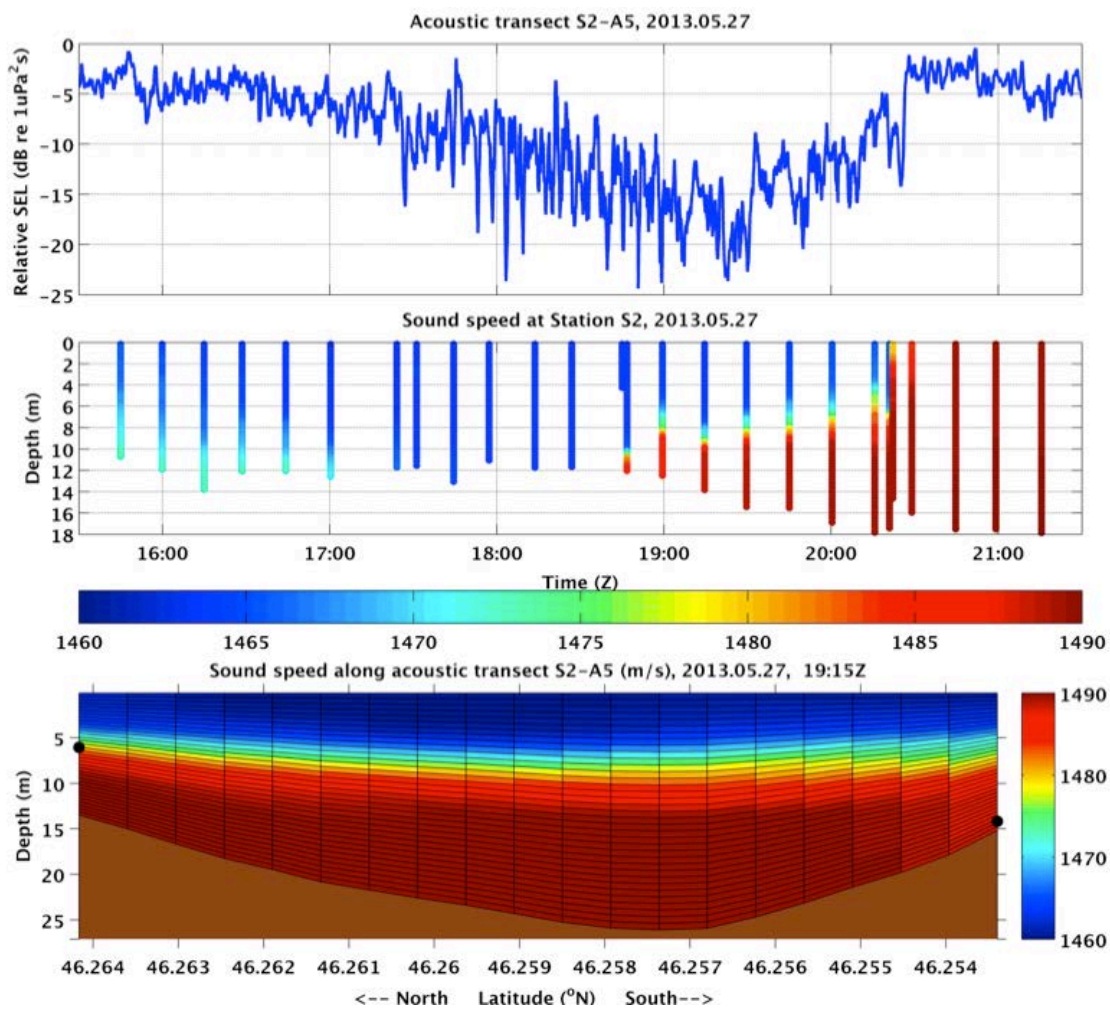

Fig. 3. Flood from 1530 to 2130 on May 27: (a) Relative SEL (dB re 1 μPa²-sec) vs. time (hr); (b) sound speed (m/s) vs. depth (m) and time (hr) observed at S2; (c) modeled sound speed (m/s) vs. depth (m) and range (deg. latitude) along the acoustic transect between S2 and A5.

The hypothesis, yet to be completely verified by acoustic modeling, is as follows: The acoustic transect is initially composed entirely of isospeed fresh water which supports the SEL observed prior to 1700, followed by the advance of the salt wedge along the bottom of the shipping channel; the salt wedge gradually fills the channel and then rises in the water column against the outward flow of fresh water. The denser salt water has a higher sound speed than the fresh water above it; this difference in sound speed causes acoustic refraction along the acoustic path resulting in a slowly increasing amount of acoustic energy to be refracted up and away from the receiver at A5 from 1700 to 1930. Some of the acoustic signal energy initially received at A5 is trapped in the thinning fresh water layer above the advancing salt wedge and above the receiving hydrophone at A5. When the salt wedge front passes the acoustic source at ~1930Z, the strong sound speed gradient in which the acoustic source is located causes the greatest degree of refraction of the entire period.As the salt wedge continues to fill the water column between source and receiver, eventually displacing the fresh water layer at the surface, the observed signal energy level recovers during a relatively short 1-hour period as minimal refraction and scattering losses are again observed, similar to conditions at the beginning of the observation period.

Besides the refractive effects of the salt wedge, note also that SEL variance increases between 1530 and 2030Z as the salt wedge front crosses the acoustic path. Potential mechanisms for this variability include (1) mixing and overturning along the salt wedge front, (2) internal waves propagating along the top of the salt wedge, and (3) subducted bubbles from the downwelling at the salt wedge front surface expression. All these mechanisms require further investigation.

A nearly identical process occurs during ebb tide as the salt wedge recedes, as seen in Fig. 2; however, during ebb, the stratification is weaker than during flood; the weaker sound speed gradient causes weaker upward refraction, resulting in a smaller decrease of 10 dB in SEL observed at Station A5.

Based upon an extensive literature search, these data constitute the first documented *in situ* acoustical observation of an estuarine salt wedge in terms of low-frequency acoustic propagation.

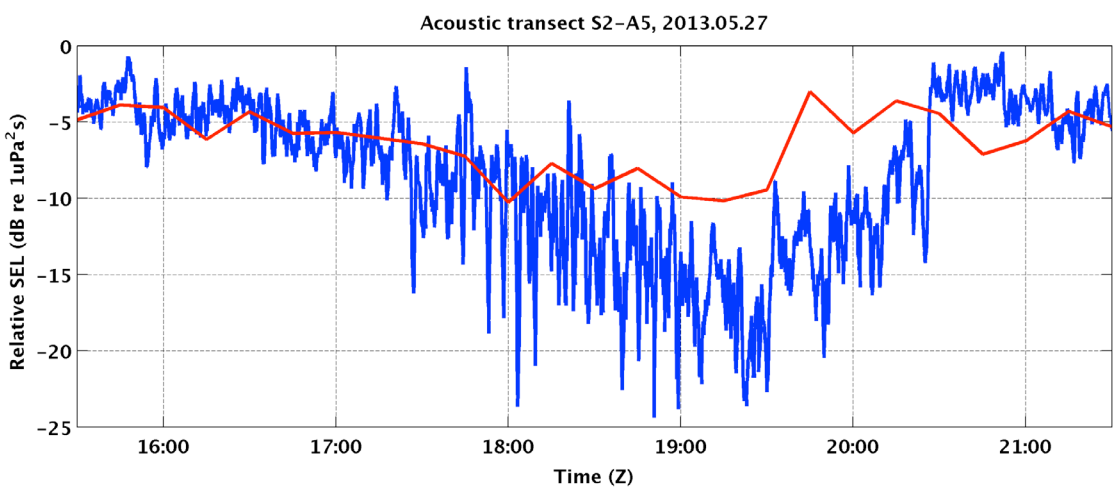

Fig. 4. Relative SEL (dB re 1 µPa2-sec) from 1530 to 2130 on May 27 (blue); modeled SEL (red).

Acoustic propagation modeling supports this interpretation and suggests the dominant physical mechanism controlling acoustic propagation through the salt wedge front. Figure 4 shows the same SEL vs. time for the flood on May 27. The red line represents acoustic propagation modeling results in terms of modeled SEL received at A5 for each of the CMOP profiles in 15-minute increments. This particular acoustic model is 2D and accounts for vertical refraction only. With the exception of the one point at 1945Z, it shows a similar trend as the data, but decreases only by about 5 dB. The salt wedge is a very much a 3D feature, so the majority of the difference between model and data is most likely due to the salt wedge refracting the acoustic energy out of plane and to the left when the salt wedge occupies the acoustic transect. Next steps in this work include 3D acoustic propagation modeling to verify this hypothesis.

Foundational to any acoustic applications in a particular environment is a proper characterization of the ambient noise field statistics. In very energetic environments like MCR, flow noise will have a large effect on the performance of any acoustic system. Flow noise occurs due to pressure fluctuations of the fluid as it flows across the hydrophone, and has been seen in other studies in the 10-1000 Hz band. Other noise sources in this band are shipping noise, surface-generated noise due to wind and breaking waves, and noise due to sediment movement. So this environment demands that flow noise be examined and placed within the context of the overall ambient noise field. Figure 5 shows the frequency dependence of the the power spectral density of the ambient noise observed at A5 averaged in 15 cm/s current speed bins. Note that the spectral slope is independent of current speed in the 20-800 Hz band. This spectral slope independence can be exploited to parameterize the spectral slope of the flow noise and generate a family of predictive curves that relates flow noise spectral level to current speed. This work is currently underway.

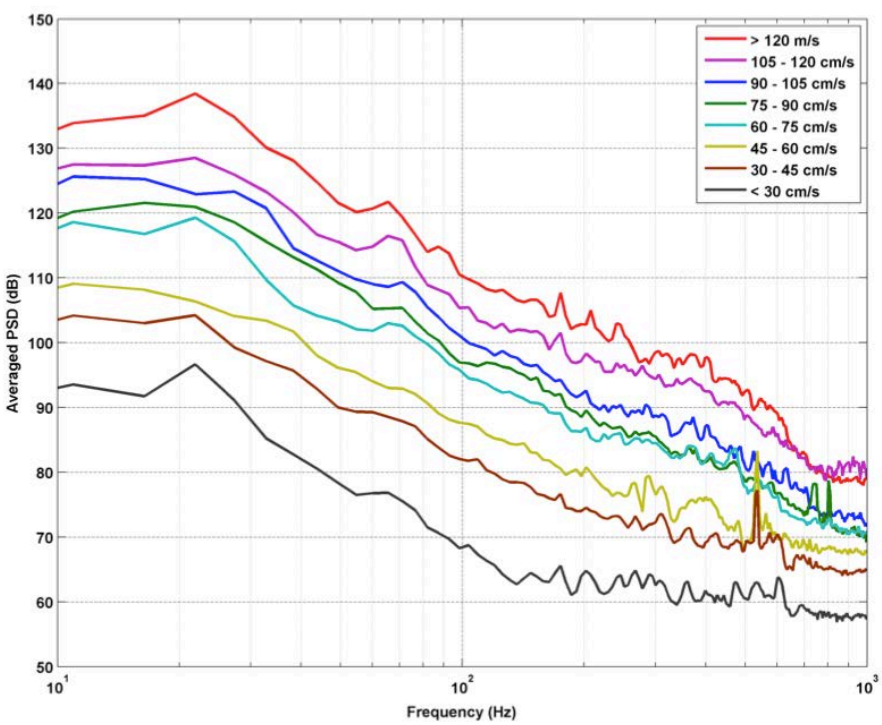

Fig. 5. Frequency dependence of the power spectral density of ambient noise observed at A5 averaged in 15 cm/s current speed bins.

IMPACT/APPLICATIONS

When correlated to the conventional riverine parameters, acoustic parameters will not only provide a deeper understanding of the riverine environment, but also the potential for new capabilities for remote persistent monitoring, rapid environmental assessment and environmental prediction.

PUBLICATIONS

Reeder, D. Benjamin (2013), "Acoustical characterization of the estuarine salt wedge", Proceedings of Meetings on Acoustics (POMA), 19/005004, doi:10.1121/1.4799122 (June).